

Expanded View Figures

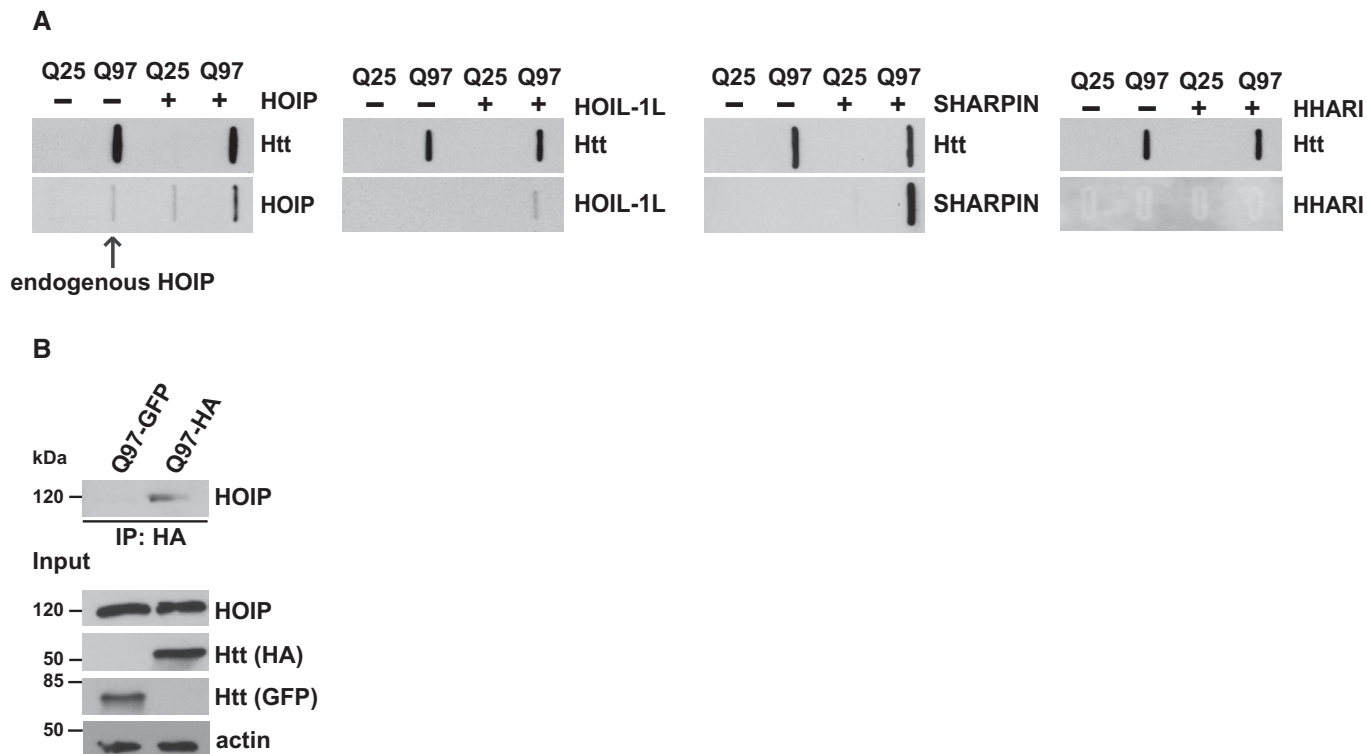


Figure EV1. HOIP, HOIL-1L, and SHARPIN co-aggregate with Htt-Q97 (related to Fig 1).

A HEK293T cells transiently co-expressing Htt-Q25 or Htt-Q97 and either HOIP, HOIL-1L, SHARPIN, or HHARI were analyzed by the filter retardation assays. Aggregated proteins retained by cellulose acetate membranes were detected by Western blotting.

B Endogenous HOIP interacts with soluble Htt-Q97. HEK293T cells were transfected with Htt-Q97-HA or Htt-Q97-GFP (as a control for specific immunoprecipitation of HA-tagged Htt-Q97). Cells were lysed with 1% Triton X-100, followed by an immunoprecipitation of Htt via the HA tag. Immunoprecipitated proteins were analyzed by Western blotting using an anti-HOIP antibody.

Source data are available online for this figure.

Figure EV2. M1 ubiquitin-specific signals occur at Htt-polyQ aggregates and are absent in HOIP-deficient cells (related to Fig 2).

A SH-SY5Y cells expressing Htt-Q25-GFP (upper panel) or Htt-Q97-GFP (lower panel) were stained for M1 ubiquitin (red) and DAPI (blue). Scale bar, 10 μ m.

B, C M1-linked ubiquitin co-localizes with Htt-polyQ aggregates in R6/2 mouse cortex and striatum (B) and human HD frontal cortex (C). Autofluorescent lipofuscin appears in the green channel in human brain. Scale bar, 20 μ m (B), 10 μ m (C).

D HAP1 WT (control) or HOIP KO HAP1 cells expressing Htt-Q97-GFP (green) were stained for M1 ubiquitin (red) and DAPI (blue). Scale bar, 10 μ m.

E Quantification of ubiquitin chains associated with SDS-insoluble Htt-Q97 from HEK293T cells by mass spectrometry (1: M1, 2: K11, 3: K48, and 4: K63). The standard error is shown with error bars ($n = 3$).

F Extracted chromatograms from the M1 ubiquitin measurements. Upper panels show the quantification of the ubiquitin chain peptide, while the lower panels show the spiked in reference peptide used for quantification. Panels 1 and 3 show an example of Htt-Q97, and panels 2 and 4 show an example of Htt-Q97 + LUBAC. Above each peak, the retention time and mass error are shown. Below the panels a legend identifying the product ions observed and used for quantification is shown.

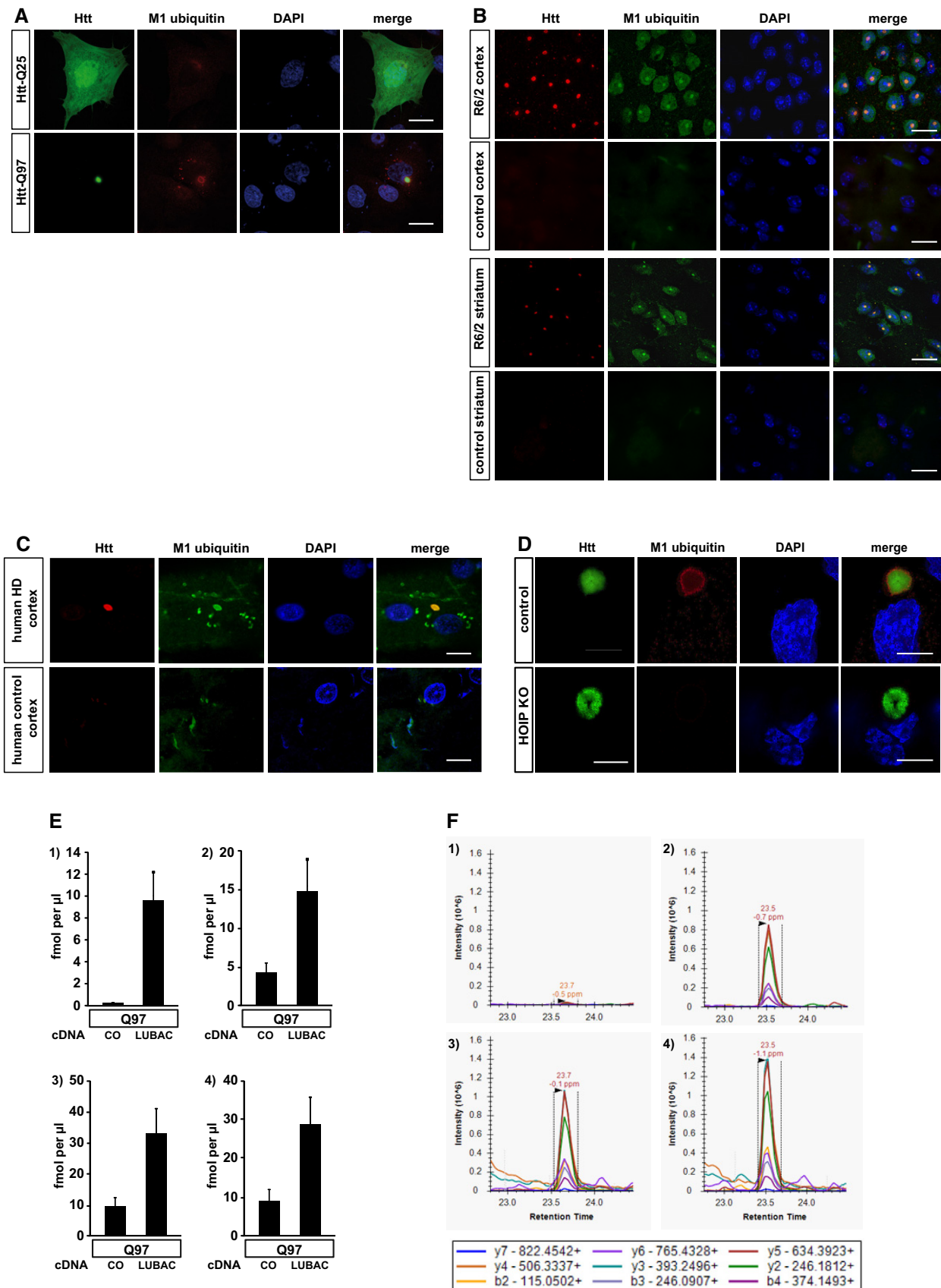


Figure EV2.

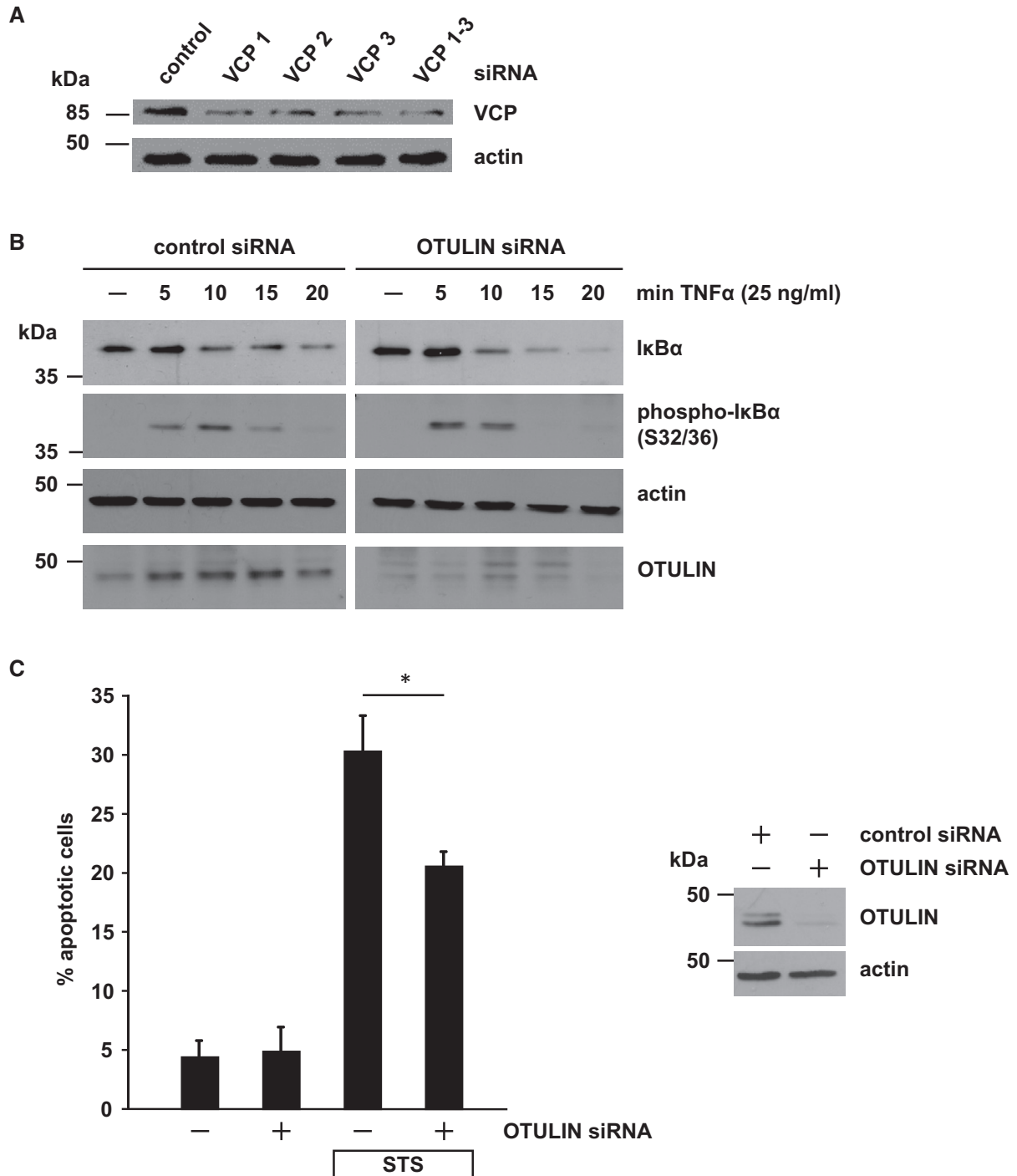


Figure EV3. OTULIN silencing protects neuronal cells from apoptotic cell death (related to Fig 4).

A Partial silencing of VCP/p97 in SH-SY5Y cells by three different siRNAs. Cells were harvested 48 h after transfection of control or VCP/p97-specific siRNAs and analyzed by immunoblotting.

B Decreased OTULIN expression promotes NF-κB activation. Degradation of IκBα or phospho-IκBα after TNF-α treatment (25 ng/ml) of SH-SY5Y cells transfected with control siRNA or OTULIN siRNA was visualized by immunoblotting using the indicated antibodies.

C OTULIN RNA interference decreases staurosporine-induced cell death. SH-SY5Y cells were treated with staurosporine (STS, 1 μM, 3 h) 2 days after transfection with control siRNA or OTULIN siRNA. Apoptotic cell death was quantified by immunocytochemistry using an antibody against active caspase-3. Data are displayed as mean ± SD and were analyzed by a Mann-Whitney U-test (**P* ≤ 0.05), *n* = 4.

Source data are available online for this figure.

Figure EV4. Endogenous NEMO and Optineurin are recruited to Htt-Q97 (related to Fig 4).

- A, B SH-SY5Y cells expressing Htt-Q25-GFP (upper panel) or Htt-Q97-GFP (lower panel) were stained for (A) NEMO (red) or (B) Optineurin (red) and DAPI (blue). Scale bar, 10 μ m.
- C, D Htt-Q25- or Htt-Q97-expressing HEK293T were analyzed by filter retardation assays. Both endogenous NEMO (C) and Optineurin (D) are retained on a cellulose acetate membrane together with SDS-insoluble Htt-Q97.
- E HOIP is required to recruit NEMO to Htt-Q97. NEMO (red) and Htt-Q97-GFP (green) were analyzed by immunocytochemistry in WT HAP1 cells (control), HOIP KO HAP1 cells, or HOIP KO HAP1 cells reconstituted with HOIP. DAPI (blue). Scale bar, 10 μ m.

Source data are available online for this figure.

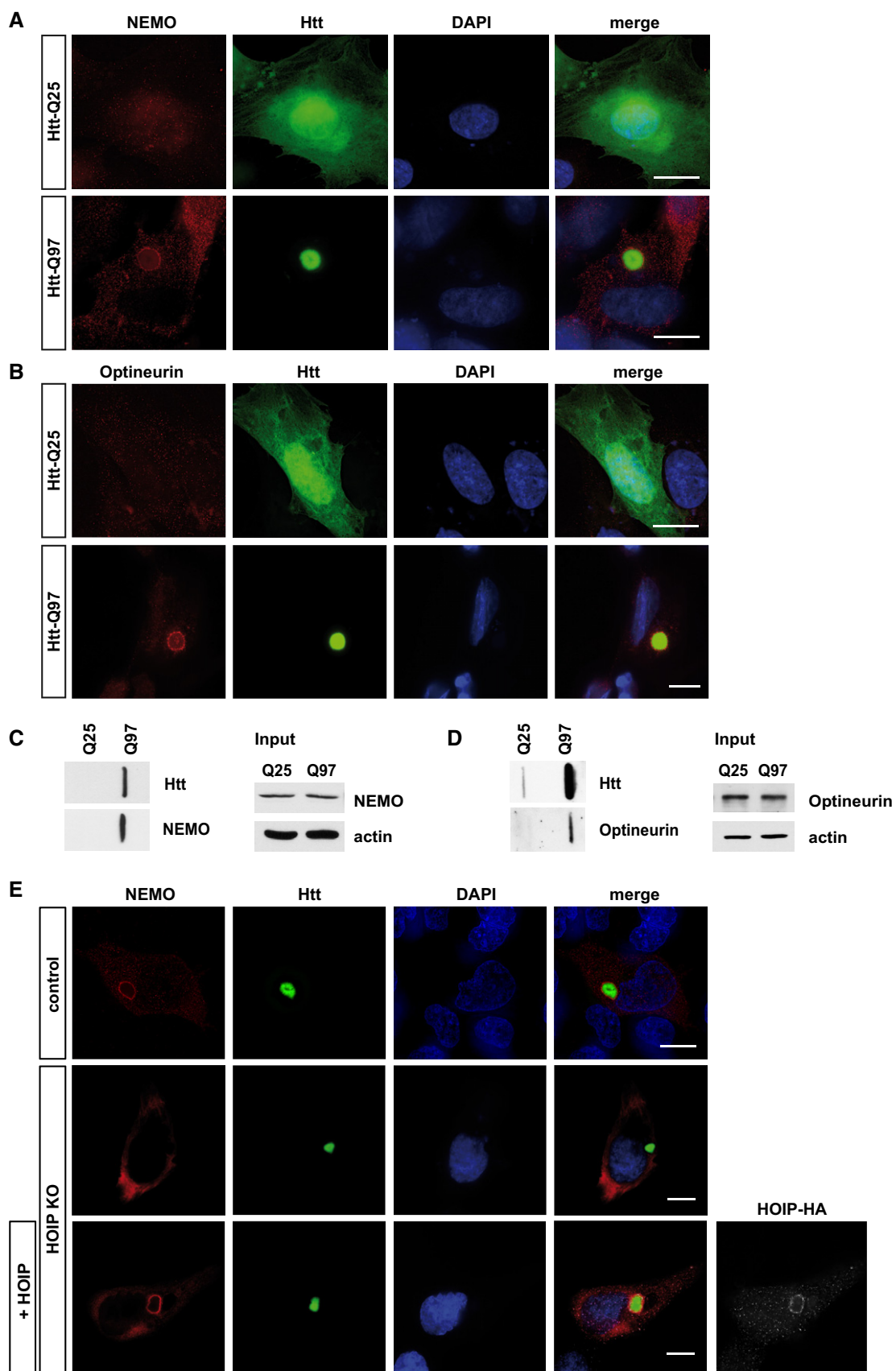
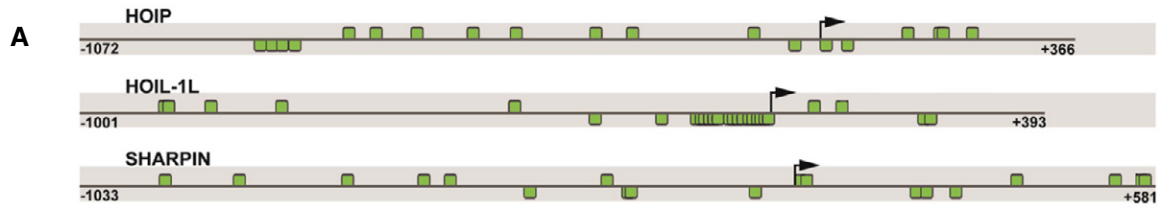


Figure EV4.

Figure EV5. Presence of highly conserved SP1 binding sites in LUBAC component genes (related to Figs 5 and 6).

- A *In silico* promoter analysis of HOIP, HOIL-1L, and SHARPIN. Promoter sequence of human HOIP, HOIL-1L, and SHARPIN showing SP1 binding sites. The black arrow indicates the transcription start site (TSS), and the positions are denoted relative to the TSS. Predicted SP1 binding sites are highlighted by green boxes. Binding sites above each line are located on the plus strand, whereas binding sites below the line are on the minus strand.
- B Species conservation of V\$SP1F binding sites in the promoter sequences of HOIL, HOIL-1L, and SHARPIN (*relative to the transcriptional start site).
- C SDS-insoluble SOD1-G85R, TDP-43-Q331K, and Htt-Q97-HA are modified by linear ubiquitin chains. HEK293T cells expressing Htt-Q97-HA, SOD1-G85R-HA, or TDP-43-Q331K-HA were lysed under denaturing conditions in 1.5% SDS. After centrifugation, the pellets containing the SDS-insoluble aggregates (SDS-insoluble fraction) were dissolved in formic acid. Formic acid-dissolved aggregates were analyzed by immunoblotting using the M1 ubiquitin-specific 1F11/3F5/Y102L antibody.

Source data are available online for this figure.



B

Gene Symbol	Matrix	Position in human promoter* [bp]	Number of species
HOIP	V\$TIEG.01	-817 to -801	4
	V\$SP1.01	-800 to -784	9
	V\$SP1.01	-785 to -769	10
	V\$GC.01	-689 to -673	8
	V\$GC.01	-650 to -634	8
	V\$SP1.02	-591 to -575	8
	V\$SP1.03	-333 to -317	6
	V\$GC.01	-105 to -89	10
	V\$SP4.01	-46 to -30	7
	V\$SP1.02	-1 to +15	9
	V\$GC.01	+30 to +46	10
	V\$SP1.03	+117 to +133	4
HOIL-1L	V\$SP1.03	-817 to -801	4
	V\$SP1.01	-36 to -20	5
	V\$SP1.03	-13 to +3	5
SHARPIN	V\$SP4.01	-808 to -792	4
	V\$SP1.01	-542 to -526	5
	V\$SP1.03	-504 to -488	7
	V\$SP4.01	-389 to -373	8
	V\$SP2.01	-278 to -262	5
	V\$SP1.03	-248 to -232	6
	V\$SP4.01	-64 to -48	8

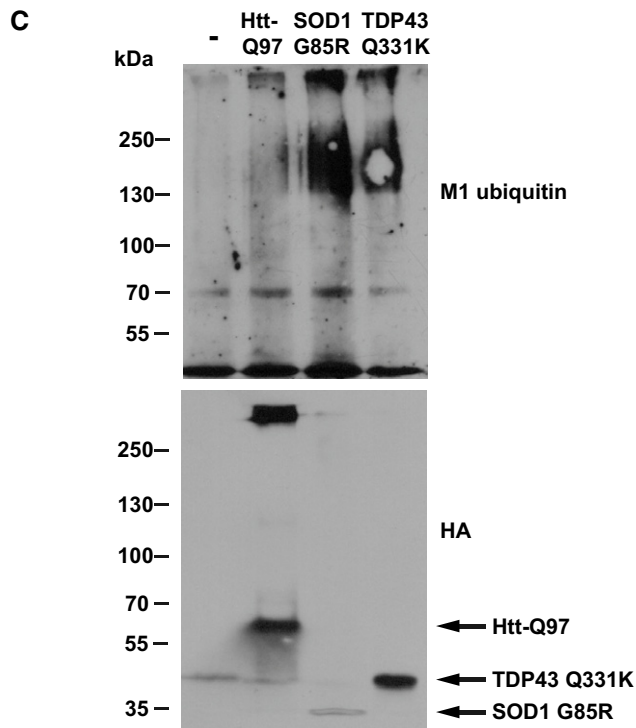


Figure EV5.